

## Three-Dimensional Numerical Modeling of the Indirect Band-to-Band Tunneling in MOSFET's

Y.Odake, K.Kurimoto and S.Odanaka

Semiconductor Research Center,  
Matsushita Electric Industrial Co., Ltd.  
3-15, Yagumo-Nakamachi, Moriguchi, Osaka 570, Japan

This paper describes a three-dimensional numerical modeling of phonon assisted indirect band-to-band tunneling in MOSFET's. The three-dimensional model has been developed by considering local tunneling paths in all directions and by introducing an indirect tunneling model. This approach reveals a broadening effect of band-to-band tunneling current observed in the gate induced drain leakage current characteristics. The present model allows a quantitative prediction of the drain leakage current due to the band-to-band tunneling.

### I. Introduction

Band-to-band tunneling phenomena have been observed in thin gate oxide MOSFET's as an undesirable effect such as the gate induced drain leakage current <sup>1)</sup>. To understand this effect, a direct band-to-band tunneling model has been developed <sup>2)</sup>, which has assumed the band-to-band tunneling path based on the electric field in the direction normal to the Si-SiO<sub>2</sub> interface. However, the experimental data is found, which cannot be explained by only the electric field in the direction normal to the Si-SiO<sub>2</sub> interface, and it has been shown that the band-to-band tunneling current strongly depends on the complicated behavior of the electric field in the drain region <sup>3)</sup>.

The purpose of this paper is to describe a three-dimensional numerical model considering a broadening effect of the tunneling current in silicon MOSFET's. For the three-dimensional modeling, the local tunneling path is defined in all directions from each incident point, including the broadening effect of the tunneling current. The transmission coefficient further includes a phonon assisted indirect tunneling effect <sup>4)</sup> and phonon scattering effect <sup>5)</sup>. The model allows quantitative prediction of the drain leakage current due to the band-to-band tunneling.

### II. Modeling

One of major features of this model is to calculate independently local tunneling current in all directions from each incident point to include the broadening effect of the tunneling current. As shown in Figure 1, the band-to-band tunneling process is calculated between an incident potential surface  $\Phi_{in}$  and a transit potential surface  $\Phi_{tr}$ , where the difference of energy is equal to the band gap. Electrons tunnel through the forbidden band from the top of valence band at  $\Phi_{in}$  to the bottom of conduction band at  $\Phi_{tr}$ . At each tunneling path, the local incident current and transmission coefficient are calculated. Figure 2 illustrates for the local incident current model at each local tunneling path. The previous one-dimensional model is also illustrated in Figure 3. There is a significant difference between two models. We assume that the incident electrons in a small area  $dSi$  travel from an incident point  $X_i$  in  $dSi$ . Under this assumption, the solid angle  $d\Omega$  is defined from the incident point  $X_i$  in  $dSi$  toward  $dSt$  in the real space. In the momentum space, the volume of spherical shell cut off by  $d\Omega$  corresponds to the number of the quantum states of the local incident electrons because they are considered to be free carriers with reduced effective mass in the tunneling process <sup>5), 6)</sup>. In this case, the

local incident current can be expressed as

$$dJ_v(E) = \left( \frac{p^2 dp}{4\pi^3 \hbar^3} \right) \cdot \left( \frac{p}{m^*} \right) \cdot [F_v(E) \{1 - F_c(E)\}] \quad (1)$$

where  $m^*$  is the reduced effective mass of  $0.2m_e$  and  $F_v(E)$  and  $F_c(E)$  are Fermi-Dirac distributions in the valence band and conduction band, respectively. The momentum of the incident electrons is estimated to be  $p = \{2m^*(E_v - E)\}^{1/2}$  and  $dp = \{m^*/2(E_v - E)\}^{1/2} dE$ , respectively, where  $E_v$  is the upper limit of energy level and  $dE$  is the differential energy of about  $0.04$  eV in our simulation.

Another feature of this model is to consider the indirect band-to-band tunneling process for accurate simulations in silicon devices. When the solid angle  $d\Omega$  is small enough for the incident electrons in  $d\Omega$  to be in the direction of the tunneling path, we can assume that the transverse momentum is equal to zero. Under this assumption, an indirect transmission coefficient given by Keldysh<sup>4)</sup> is modified as follows:

$$T = \alpha M^2 V F^{-1/2} dS t^{-1} \times \left[ (\bar{n} + 1) \cdot \exp\left\{-\pi m^* \frac{1}{2} (E_g + \hbar\omega)^{3/2} / 2\sqrt{2} \hbar F\right\} + \bar{n} \cdot \exp\left\{-\pi m^* \frac{1}{2} (E_g - \hbar\omega)^{3/2} / 2\sqrt{2} \hbar F\right\} \right] \quad (2)$$

where  $\alpha \equiv m^* \frac{3}{4} \pi^{1/2} / 2^{3/4} \hbar^{3/2} E_g^{3/4}$  and the phonon energy  $\hbar\omega$  is  $5.8 \times 10^{-2}$  eV.  $M^2 V$  is the phonon matrix element of  $1.3 \times 10^{-46}$  erg<sup>2</sup>cm<sup>3</sup> and  $\bar{n}$  is the phonon occupation number, which is represented as  $\bar{n} = \{\exp(\hbar\omega/kT) - 1\}^{-1}$  using thermal energy  $kT$ . In the expression(2), an average electric field  $F = E_g / |X_i - X_f|$  along each tunneling path and the parabolic potential barrier approximation are further assumed.

Moreover, the phonon scattering effect in the indirect tunneling process is induced<sup>5)</sup>

$$S(E) = \left( \sqrt{2m^* / E_g F} \right) dS t / 4\pi^2 \hbar \times \left[ 1 - \exp\left\{-\pi \sqrt{2m^* E_g} (E - E_c) / \hbar F\right\} \right] \quad (3)$$

where  $E_c$  is the lower limit of energy level. Using the equations (1)-(3), the local tunneling current is modeled at each tunneling path as follows:

$$dJ_{v \rightarrow c}(E) = dJ_v(E) \cdot T \cdot S(E) \quad (4)$$

Summing up the values of the local tunneling currents at all tunneling paths, the total tunneling current distributions are derived. The local tunneling current from the conduction band to the valence band is similarly given. This model has been implemented into a three-dimensional device simulator SMART<sup>7)</sup> in a self-consistent manner.

### III. Results and Discussions

An experimental data, which demonstrates the broadening effect of band-to-band tunneling current, is shown in Figure 4. Figure 4 shows the drain leakage current induced at the gate voltage  $V_g < 0$  in the wide range of the drain voltage. The device is a conventional n-MOSFET with the gate oxide thickness of  $7$  nm. A source/drain is formed by an arsenic implant with a dose of  $6.0 \times 10^{15}$  ions/cm<sup>2</sup> at  $80$  KeV. The closed circles and triangles in Figure 4 correspond to the experimental data and simulations, respectively, when the drain-gate voltage  $V_{dg}$  is applied to  $5.0$  V. The results indicate that even at constant  $V_{dg}$  the drain leakage current decreases if the drain voltage is decreased.

To make this phenomenon more clear, the drain leakage currents at  $V_{dg} = 5.0$  V are plotted in Figure 5 and they are compared with the results calculated using the previous model<sup>2)</sup>. The drain currents are normalized by the value of the drain current at  $V_d = 4.0$  V, respectively. At the constant  $V_{dg}$ , the drain leakage currents calculated using the previous model have little dependence on the drain voltage. However, the experimental data shows that the drain leakage current increases as the drain voltage increases. To understand this result, we can see simulation results of the electric field and carrier generation distributions due to the band-to-band tunneling. Figure 6 shows the simulations of the normal and lateral electric fields at the Si-SiO<sub>2</sub> interface, subject to  $V_d = 0.5$  V and  $V_d = 4.0$  V at the constant  $V_{dg} = 5.0$  V. Although the peak of normal electric field is kept to be constant in both cases, the lateral electric field becomes high as the drain voltage increases. Moreover, Figure 7(a) and (b) shows the simulations of potential distributions and carrier generation distributions at the same applied

biases as Figure 6. As shown in Figure 7(a) and (b), at the high drain voltage ( $V_d=4.0V$ ), the band bending is induced in the lateral direction and the tunneling current is generated at larger region. The peak of carrier generation due to the band-to-band tunneling at the high drain voltage ( $V_d=4.0V$ ) is more than  $10^2$  times larger than that at the low drain voltage ( $V_d=0.5V$ ). These results are consistent with the experimental data shown in Figure 5, which indicates about  $10^3$  times difference of the drain leakage current between at  $V_d=0.5V$  and  $V_d=4.0V$ . The present model considers the broadening effect of band-to-band tunneling and hence the results calculated using the present model gives a good agreement with the experimental data.

To further achieve the quantitative simulation, an indirect tunneling model is introduced. The present model is verified in Figure 8 by the experimental data of  $I_d$ - $V_d$  characteristics for the conventional n-MOSFET. It is compared with the result calculated using the direct tunneling model with the transmission coefficient given by the WKB approximation. The direct tunneling model overestimates the experimental data and the indirect tunneling model gives better prediction for  $I_d$ - $V_d$  characteristics. This is due to the difference of the transmission coefficient between two models. As shown in Figure 9, the indirect transmission coefficient is reduced to about 1/100 of that calculated using the direct tunneling model. The phonon scattering effect has little impact on the total transmission coefficient but it reduces the tunneling probability by half.

#### IV. Conclusion

A three-dimensional numerical model of the band-to-band tunneling has been developed by considering the local tunneling paths in all directions and by introducing the indirect tunneling model. The model includes the broadening effect of the band-to-band tunneling and gives a quantitative simulation of the band-to-band tunneling phenomena in the wide range of the drain and gate voltages.

#### Acknowledgment

The authors would like to thank Dr.T.Takemoto and Y.Terui for their encouragement during this work. The authors also thank H.Umimoto, A.Hiroki, K.Ohe and K.Moriyama for helpful discussions.

#### References

- 1) T.Y.Chan, J.Chen, P.K.Ko and C.Hu IEDM Tech. Dig., p.718, 1987.
- 2) T.Endoh, R.Shirota, M.Momodomi and F.Masuoka; IEEE Trans. Electron Device **ED-37**, (1990) 665.
- 3) K.Kurimoto, Y.Odake and S.Odanaka ; IEDM Tech. Dig., p.621, 1989.
- 4) L.V.Keldysh, Sov. Phys. JETP **34(7)**, (1958) 665.
- 5) E.O.Kane, J. Appl. Phys. **32(1)**, (1961) 83.
- 6) J.L.Moll,"*Physics of Semiconductors*," McGraw-Hill, New York, p.249, 1964.
- 7) S.Odanaka, M.Wakabayashi, H.Umimoto, A.Hiroki, K.Ohe, K.Moriyama, H.Iwasaki and H.Esaki ; ISCAS Proc., p.534, 1987.

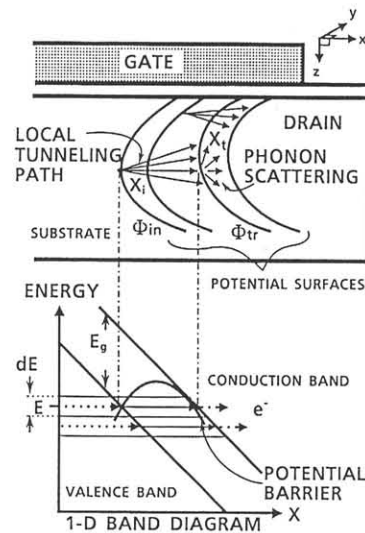


Figure 1. An illustration for new three-dimensional indirect band-to-band tunneling model. The incident current and transmission coefficient are calculated at each tunneling path in three dimensions to include a broadening effect of the band-to-band tunneling.

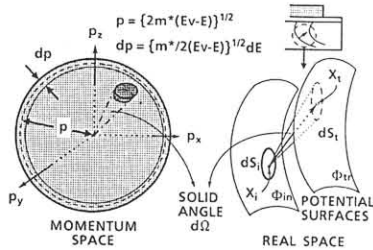


Figure 2. A schematic illustration for the local incident current model

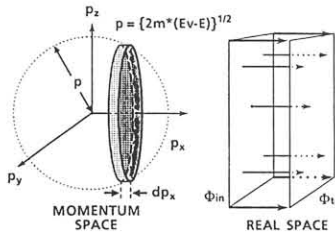


Figure 3. A schematic illustration for the local incident current of a one-dimensional model.

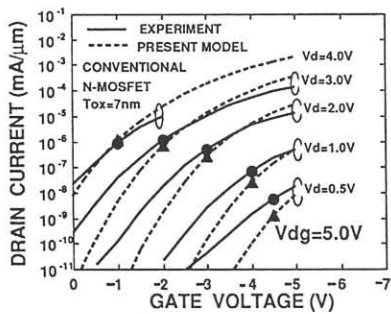


Figure 4. The drain leakage currents induced at the gate voltage  $V_g < 0$  in the wide range of the drain voltage. The closed circles and triangles correspond to the experimental data and simulations at the constant  $V_{dg} = 5.0V$ , respectively.

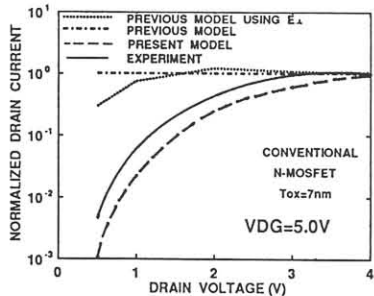


Figure 5. The experimental data and simulations using the present model for the drain leakage currents at  $V_{dg} = 5.0V$ . They are compared with the results from the previous model <sup>2)</sup> and the previous model using the value of electric field in the direction normal to the Si-SiO<sub>2</sub> interface, which is calculated by device simulators. The drain leakage currents are normalized by the value of drain leakage current at  $V_d = 4.0V$ .

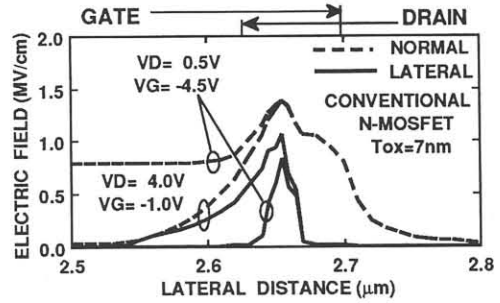


Figure 6. Simulations of the lateral and normal electric fields at the Si-SiO<sub>2</sub> interface. The bias conditions are  $V_d = 4.0V$  and  $V_d = 0.5V$  at the constant  $V_{dg} = 5.0V$ .

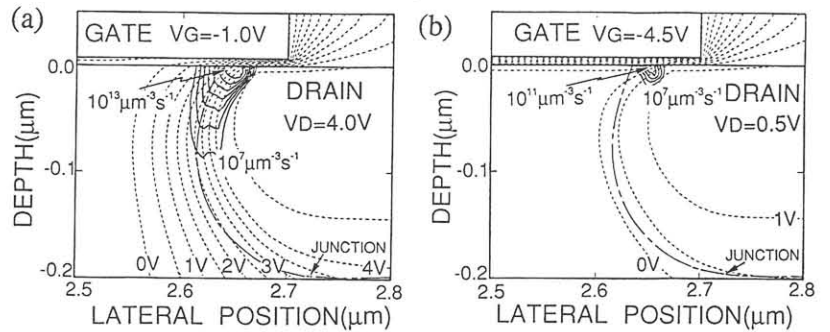


Figure 7(a) and (b). Simulations of carrier generation distributions due to the band-to-band tunneling calculated using the present model and potential distributions. (a)  $V_d = 4.0V$ . (b)  $V_d = 0.5V$ .

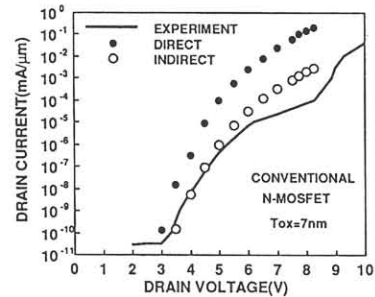


Figure 8. Comparison of the drain leakage current characteristics between simulations and the experimental data for the conventional n-MOSFET. Open and closed circles correspond to the results calculated using the indirect and direct tunneling models, respectively.

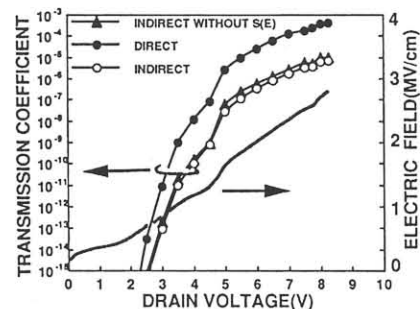


Figure 9. Comparisons of transmission coefficient of the direct tunneling model, indirect tunneling model and indirect model without phonon scattering effect as a function of the drain voltage for the conventional n-MOSFET.